Chapter 7

Load Frequency Control of Stand-alone PV-Wind hybrid power system

7.1 Introduction

The detailed mathematical modeling of PV and Wind based generation has been studied with equation and model-based implementation of PV and wind power generation. An FLC-based MPPT algorithm was implemented to improve the performance of the proposed PV-wind hybrid power system shown in Figure 7.1 under varying environmental and load conditions. The FLC-based MPPT algorithm maintains the DC bus-bar voltage constant irrespective of different test conditions. The constant DC voltage is inputted to the Voltage Source Inverter (VSI) which converts DC into AC. VSI plays a critical role in stand-alone PV-Wind hybrid power system as it enables the control over AC output voltage and frequency. So, the LFC techniques are implemented in the inverter control implementation to achieve LFC of the system. This chapter highlights the control implementation under different conditions and the performance is evaluated with the grid code as a benchmark for output voltage and frequency.

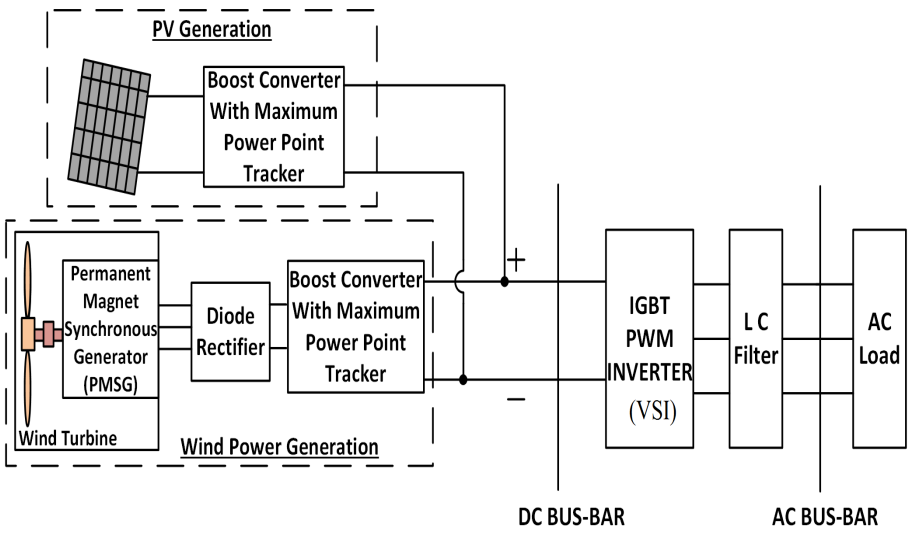

FIGURE 7.1: Block diagram of PV-Wind Hybrid Power System.

7.2 Stand-alone PV Wind Hybrid Power System

The technology to harness power from the Renewable Energy Sources (RES) such as the Wind, Photovoltaic (PV), Fuel-cell etc.. is growing exponentially. This technology is gaining importance in order to meet the gap between energy demand and generation. With the impact of global warming, a clean and green energy generation technique has evolved to control the carbon emission knows as RES generation. From different RES generation's Wind Generation and PV based generation are well-established technologies all over the world. They provide a wide opportunity to utilize solar and wind resources available at no cost. The RES generation are selected depending on the geographical location and environmental conditions. It has an unpredictable nature of generation as the power generated by RES totally depend on the environmental conditions. In order to have a sustainable power generation, a Hybrid RES power generation technique is employed. The Hybrid Power system is a combination of different forms of Renewable Energy Sources (RES). The RES like Fuel Cell, Wind, Photovoltaic (PV) etc. are integrated together to have a better eco-friendly solution for energy generation. Such generations are advantageous as the power generated from RES in the hybrid power system will be complementing the other source, thereby the storage reserves are reduced. They have low maintenance, increases reliability and efficiency of the system. In order to select RES for the stand-alone hybrid power system, the knowledge of environmental

conditions is essential. In the location having rich solar irradiance level and moderate wind speed profile, the combination of PV-Wind hybrid power system with PV as the main source of generation and wind power as complimenting source will be suitable and increase the reliability of the hybrid system. The major drawback of the stand-alone hybrid power system is to have a stable output voltage and frequency in the standard range i.e. for a three phase AC system line voltage is 415 V at a 50Hz frequency in India [264]. To achieve the task of maintaining the output voltage and frequency constant, many researchers have proposed control strategies and different combination of power electronic converters Arafat, M.N et. al [265] has worked towards seamless transitions between grid connected and islanded mode of operation of utility inverter. A space vector PWM technique is employed to generate grid angle in order to control the inverter output voltage. Ariana, M. et. al [266] has proposed a Phase Locked Loop (PLL) based inverter voltage control of islanded microgrid. A voltage, current and frequency control logic were implemented to have a stable operation of the islanded microgrid. Ozdemir, E. et. al [267] has evaluated the performance of a 7.2 kW PV generation for rural electrification. A local grid was installed to feed power to 16 houses forming a local load. An extensive analysis of the performance was reported with improved efficiency. Rong-Jong Wai et. al [268] a comparative analysis of simulation model with the real-time system was done and by the analysis, it has been concluded that the simulated model have viable results and different topologies of inverters were proposed by different researchers for stand-alone system in the literature [269–272].

The VSI provides flexibility of operation to RES generation to operate in grid-tie mode or in stand-alone mode. In grid-tie mode the control logic of the VSI is to maintain the magnitude of the output voltage and frequency in reference to the grid, In stand-alone mode, VSI has to maintain the load voltage and frequency within the specified limits in reference to a set value. Various researchers have proposed different control techniques for the VSI for stand-alone or grid-connected operation. The output voltage and frequency of the RES generation are controlled by the VSI with an appropriate control scheme. The selection of control scheme depends on the mode of operation of hybrid power system, different control

schemes are based on PLL, droop characteristics, Fuzzy logic based etc.. were proposed in the literature for different combination of RES generation with diesel generator or grid-tie systems [273–276]. With an appropriate control scheme of VSI, the power flow i.e. active and reactive power, voltage and frequency of the RES generation can be controlled [277].

It has been observed that a number of researchers have worked on different combinations of PV, the wind, other RES generation connected to the conventional power system in terms of improving the Maximum Power Point Tracking (MPPT) algorithm, optimal placement of PV-wind or a combination of RES sources, energy management system, and optimization. In grid-connected mode the PLL based inverter control technique the phase angle θ is computed from the load voltage measured which in turn used to compute the control signal to control output AC voltage and frequency and in stand-alone mode computation of reference phase angle θ and to maintain output voltage and frequency constant requires different loops of control implementation. In order to have an enhanced control, a discrete PLL is employed instead of conventional PLL to control the inverter. The input to the discrete PLL control are the desired frequency and phase angle. The value of the control parameter θ is computed with respected to the desired frequency and phase angle. which makes the design of control logic simpler for implementation. The other technique for LFC is Droop Characteristics based control. The droop characteristics based technique enables the power control with respect to frequency. The block diagram of the system is shown in Figure 7.2.

In this chapter a comparative analysis of the VSI control strategy implemented using PLL based voltage control scheme and droop characteristics based control strategy are analyzed for their effectiveness in controlling the load voltage and frequency with respective to change in load conditions for a 20 KW stand-alone operation of PV-Wind hybrid system feeding an AC load.

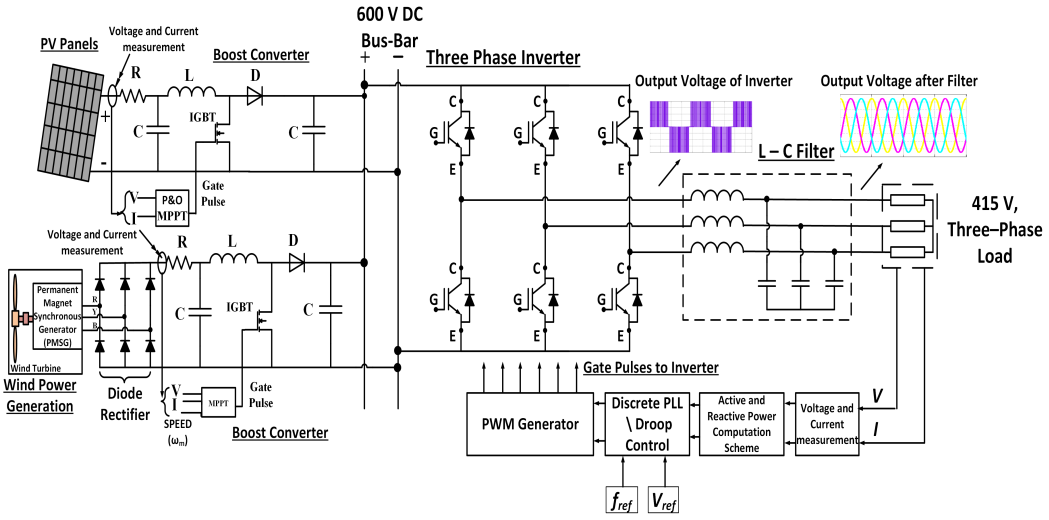

FIGURE 7.2: Block Diagram of PV-Wind hybrid Power system with DC load

7.3 A Discrete PLL based LFC of Autonomous PV-Wind Hybrid power system

The inverter plays a key role in the hybrid power system. In the stand-alone application the load voltage, the frequency is controlled and maintained constant using an inverter. The proposed control logic for the voltage regulated inverter maintains the output voltage and frequency constant irrespective of change in wind speed, solar irradiation levels, and load condition. The rectified and boosted DC voltage from the PV, the Wind is applied as an input to the inverter. The schematic diagram of Voltage regulated inverter is shown in Figure 7.3. The important aspect of voltage regulated inverter is to compute the control signals

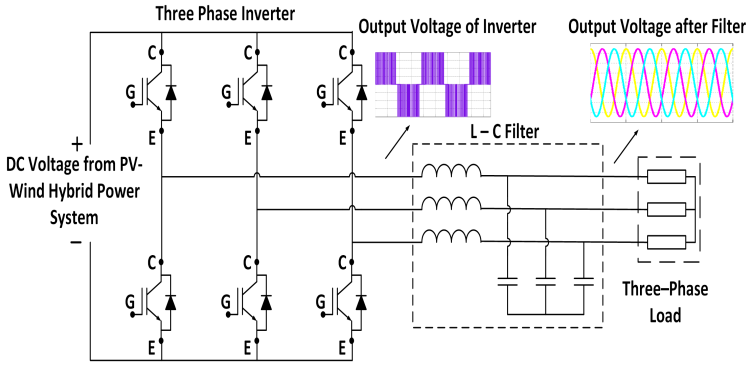

FIGURE 7.3: Voltage Regulated inverter

by minimizing the error between the measured and reference output voltage by generating the PWM

triggering pulses and to the maintain output voltage and frequency constant. In order to achieve the task, a discrete PLL with Synchronous Reference Frame (SRF) is implemented to sense the load voltage and to generate a control signal of the inverter. The control logic schematics is graphically represented in Figure 7.4. The three-phase load voltage V_{Labc} is sensed and using Clark transformation V_{Labc} is converted in to

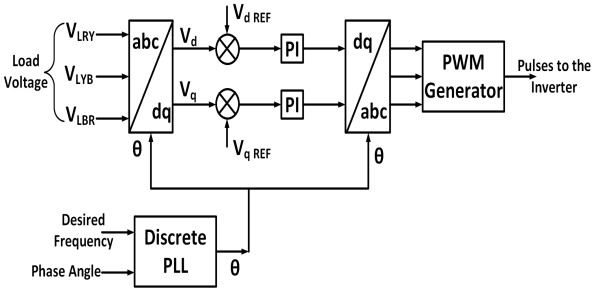

FIGURE 7.4: Block diagram of voltage regulated inverter

$V_{\alpha\beta}$ and this $V_{\alpha\beta}$ reference frame is converted into dq reference frame using (7.1) and (7.2).

$$\begin{bmatrix} V_\alpha \\ V_\beta \end{bmatrix} = \frac{2}{3} \begin{bmatrix} 1 & -\frac{1}{2} & -\frac{1}{2} \\ 0 & -\frac{\sqrt{3}}{2} & \frac{\sqrt{3}}{2} \end{bmatrix} \begin{bmatrix} V_a \\ V_b \\ V_c \end{bmatrix} \tag{7.1}$$

$$\begin{bmatrix} V_d \\ V_q \end{bmatrix} = \begin{bmatrix} cos\theta & -sin\theta \\ sin\theta & cos\theta \end{bmatrix} \begin{bmatrix} V_\alpha \\ V_\beta \end{bmatrix} \tag{7.2}$$

The angle θ is the estimated phase of the system which is computed by the discrete PLL with the given desired frequency i.e. 50 Hz and the phase angle 0^0 as shown in Figure 7.5.

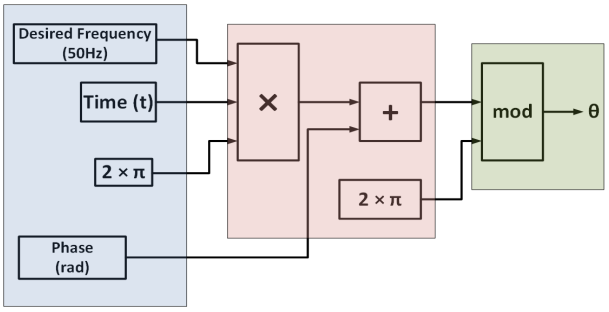

FIGURE 7.5: Block diagram of Discrete PLL

Depending on the phase estimated the control logic computes the control signal for the inverter. The V_d, V_q computed are compared with the reference $V_d = 1$, $V_q = 0$ and the error is minimized using PI controller. The control signal from PI controller is converted into abc reference frame and gating signals are generated to control the switching action of the voltage regulated inverter. With this proposed control scheme the performance of the inverter to maintain the three phase output voltage and frequency of the system constant irrespective of change in environmental, load conditions is investigated.

7.3.1 The measured data of Solar Illumination and Wind Speed

The real-time data of Solar illumination and wind speed are recorded using a Weather Monitoring System(WMS) installed at Bits-Pilani, Hyderabad campus as shown in Figure 5.10. The solar illumination and wind speed measured by the WMS are recorded using a data logger. The measured data is stored in the intervals of every 15 minutes and the data accumulated is further saved in the format of Hourly and daily. The average and maximum value of solar illumination and wind speed are measured and recorded in the said format. The historical data of average monthly maximum solar irradiation (W/m^2) and Wind Speed (m/s) are represented in a tabular format as shown in Table.7.1.

TABLE 7.1: Historical data of Monthly Average Solar illumination levels (W/m^2)

	2012		2013		2014	
	Solar Insolation (W/m^2)	Wind speed (m/s)	Solar Insolation (W/m^2)	Wind speed (m/s)	Solar Insolation (W/m^2)	Wind speed (m/s)
Jan	782	6.7	812	6.6	848	6.8
Feb	892	6.8	897	7.1	909	6.9
March	899	6.8	940	7.2	1027	6.7
April	946	8.4	968	7.4	954	7.4
May	978	8.3	1006	8.4	1041	9
June	999	9.7	1087	9.7	1076	9.3
July	1027	9.1	1036	9.9	1064	10.1
Aug	1128	8.7	1141	8.6	1141	8.3
Sep	1129	7.7	1183	6.6	1109	6.1
Oct	966	7.1	1010	6.3	990	6.2
Nov	835	6.1	913	5.9	873	6
Dec	833	6	832	6	821	6.1

From the historical data considering one-day solar illumination and wind speed data for investigating the performance of control logic implementation. The solar and wind speed data for a day are graphically represented in Figure 7.6 and Figure 7.7.

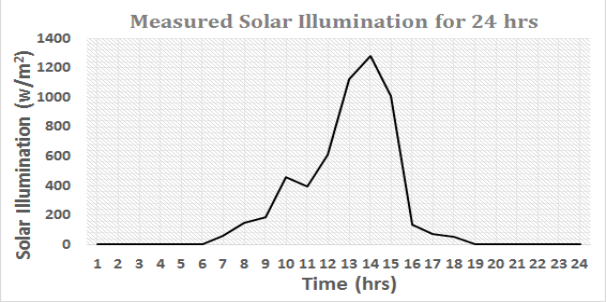

FIGURE 7.6: Solar illumination profile measured for a day

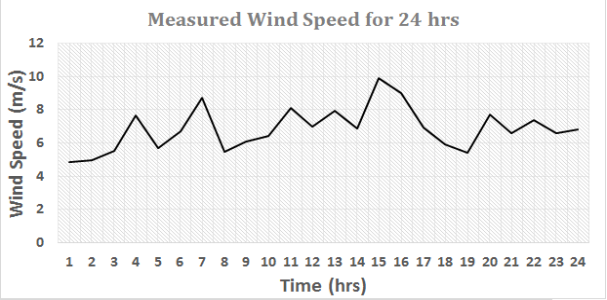

FIGURE 7.7: Wind speed profile measured for a day

Figure 7.6 shows the solar illumination recorded over a day at the location and the maximum solar illumination recorded is 1300 W / m^2. Figure 7.7 shows hourly wind speed measured at the location. The maximum wind speed measured is 10 m/s.

7.3.2 System Description and Simulation results

A 20 KW PV-Wind hybrid system with 15 KW PV, 5 KW Wind generation is implemented in MATLAB, Simulink environment. To analyze the performance of control logic, the PV-Wind hybrid power system is simulated for the following conditions

(i) Constant resistive load of 20 KW,

(ii) Varying load condition,

(iii) Increasing Load pattern and

(iv) Decreasing load pattern

(v) Constant resistive load with a 4 kW induction motor with variable load torque

the performance of voltage regulated inverter is investigated in terms of maintaining the output voltage, frequency of the system constant.

7.3.2.1 Constant resistive load of 20 kW with measured values of solar illumination and wind speed:

The performance of control logic implementation of VRI for PV-Wind hybrid power system developed in MATLAB, Simulink is investigated with the recorded data of solar illumination, wind speed as shown Figure 7.6, Figure 7.7 respectively under a constant resistive load of 20 kW. The desired control action is to maintain the output voltage and frequency of the PV-Wind hybrid system constant under varying environmental conditions with a constant load on the system.

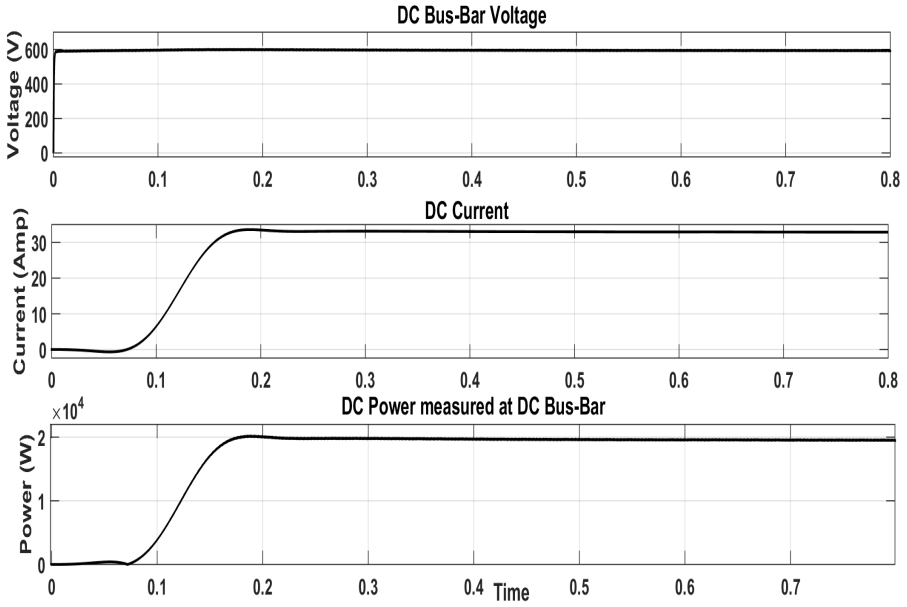

FIGURE 7.8: a) DC Bus-Bar Voltage, b) DC Bus-Bar Current, c) DC Bus-Bar power

The simulated DC Bus-Bar Voltage, Current and power are measured and graphically represented in Figure 7.8 a)- c). The system is simulated for 0.8 sec consider the scale of 0.1 sec is 1 hr as the PV based

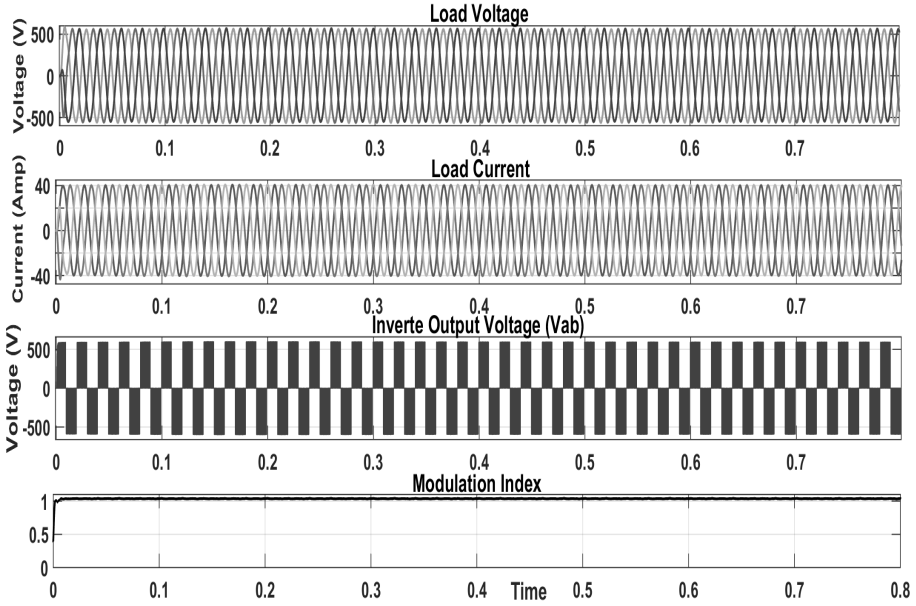

FIGURE 7.9: a) Load Voltage, b) Load Current, c) Inverter output voltage, d) Modulation index

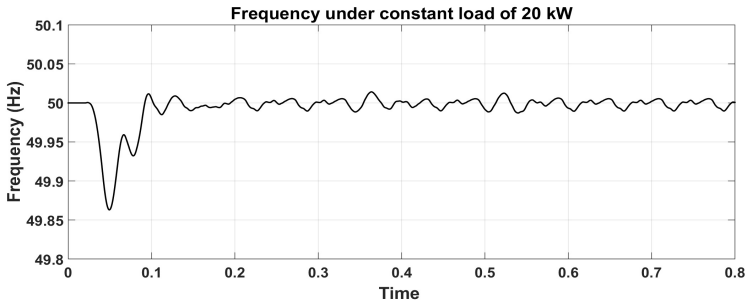

FIGURE 7.10: Frequency of the system under constant load condition

generation output is available from 8.00 am to 4.00 pm. It can be comprehended that the FLC-based MPPT controlled boost converter maintains the DC bus-bar voltage constant at 600 V and power of 20 kW from RES generation irrespective of change in environmental condition. Simulated AC Bus-Bar or load Voltage, current, inverter output Line voltage V_{ab} before filter and modulation index are plotted in Figure 7.9 a)- d). From the Figure 7.9, it is comprehended that the discrete based PLL control implementation maintained the AC bus-bar voltage constant at 415 V. The frequency of the system under constant load condition is graphically represented in Figure 7.10 and it can be concluded that the control logic implementation of inverter worked as desired by maintaining the frequency at 50 Hz. The performance of inverter is computed and tabulated as shown in Table 7.2. The efficiency of the inverter at full load unity power factor under variable environmental conditions computed is 98.01%.

TABLE 7.2: Performance of the inverter under varying environmental and constant load condition

	Voltage (V)	Current (Amp)	power(W)
DC Bus-Bar	600	34.05	20,430
AC Bus-Bar	$(578/\sqrt{2}) = 409$	$(40/\sqrt{2}) = 28.28$	$\sqrt{3} \times 409 \times 28.28 \times 1 = 20,033$
Efficiency of Inverter	$\frac{ACBus-BarPower}{DCBus-BarPower} =$	$\frac{20,033}{20430} \times 100 =$	98.01 %

7.3.2.2 Variable resistive load with measured values of solar illumination and wind speed:

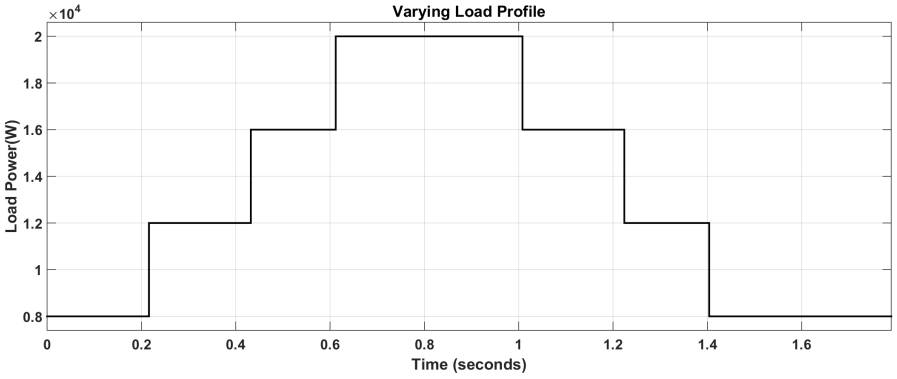

FIGURE 7.11: Varying resistive load pattern

The performance of control logic implementation of VRI for PV-Wind hybrid power system developed in MATLAB, Simulink is investigated with the recorded data of solar illumination, wind speed as shown Figure 7.6, Figure 7.7 under variable resistive load as shown in Figure 7.11. The desired control action is to maintain the output voltage and frequency of the PV-Wind hybrid system constant under varying environmental and load condition on the system. The simulated DC Bus-Bar Voltage, Current and power inputted to the inverter are measured and graphically represented in Fig. 7.12 a)- c). To have a clear understanding of the system under varying loading condition the system is simulated for 1.6 sec considering the scale of 0.1 sec is 30 min. The performance of FLC-based MPPT controlled boost converter is evaluated in terms of maintaining the DC bus-bar voltage constant at 600 V irrespective of change in environmental and load conditions.

Simulated AC Bus-Bar or load Voltage, current, inverter output Line voltage V_{ab} before filter and modulation index are plotted in Figure 7.13 a)- d). Form the Figure 7.13 it can be comprehended that the discrete based PLL control implementation maintained the AC bus-bas voltage constant irrespective of

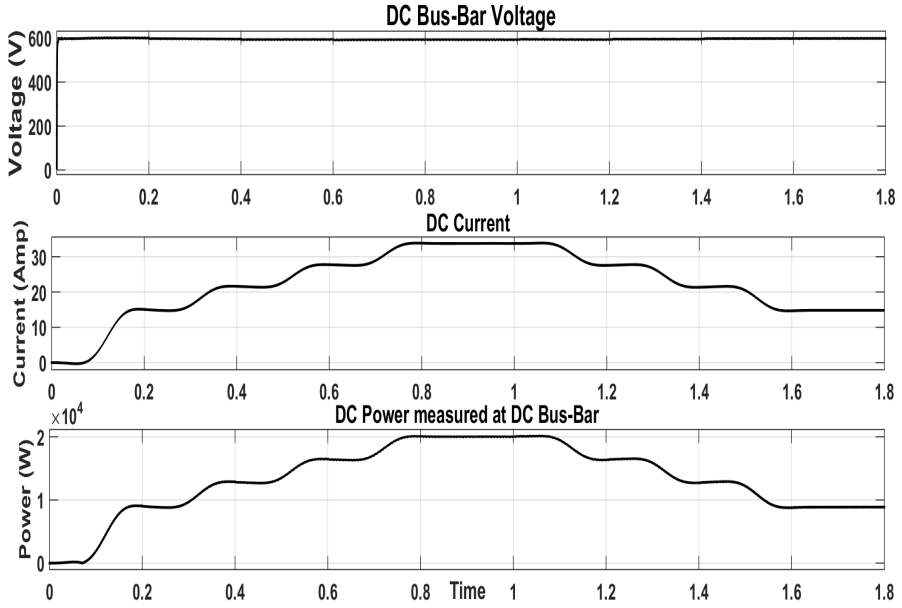

FIGURE 7.12: a) DC Bus-Bar Voltage, b) DC Bus-Bar Current, c) DC Bus-Bar power

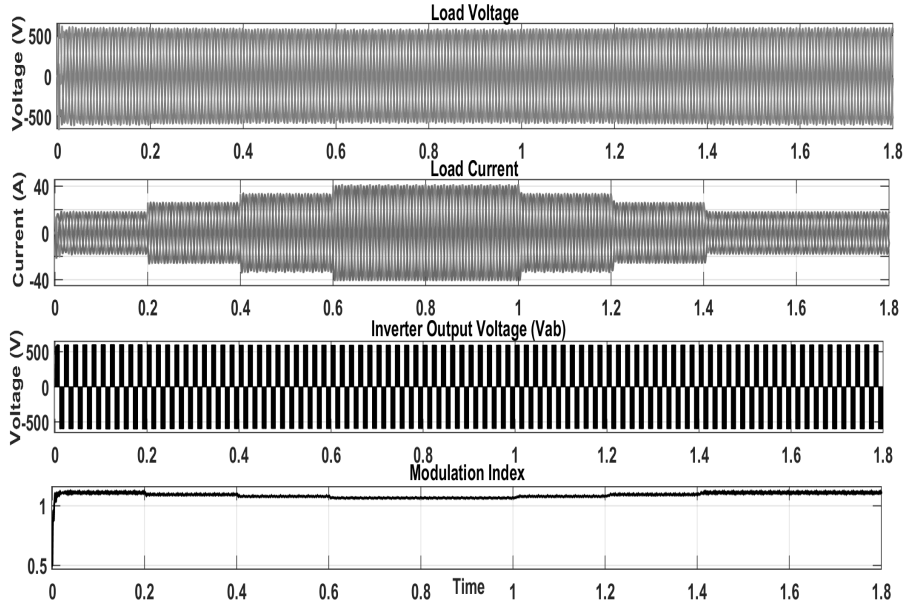

FIGURE 7.13: a) Load Voltage, b) Load Current, c) Inverter output voltage, d) Modulation index

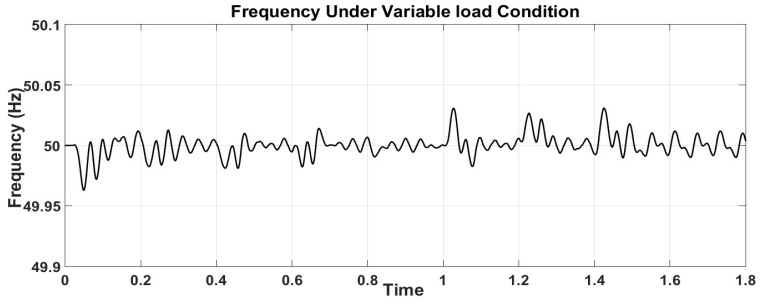

FIGURE 7.14: Frequency of the system under variable load condition

change in environmental and load conditions. The frequency of hybrid system is graphically represented in Figure 7.14 and from the plot it can be concluded that the frequency of system is maintained with in the standard limits as per grid code i.e. 50 $\pm$ 1 Hz. The performance of inverter is computed and tabulated as shown in Table 7.3.

TABLE 7.3: Performance of the Inverter under varying environmental and load condition

	DC Bus-Bar			AC Bus-Bar			
Time	Voltage (V)	Current (Amp)	Power (W)	rms Voltage (V)	rms Current (Amp)	Power (W)	Efficiency (%)
0 - 0.2 , 1.6 - 1.8	600	14.66	8,800	417	12.02	8,686	98.7
0.2 - 0.4, 1.2 - 1.4	600	21.33	12,800	417	16.97	12,263	95.8
0.4 - 0.6, 1.0 - 1.2	600	27.33	16,400	410	22.63	16,073	98.0
0.6 - 1.0	600	34.05	20,430	409	28.28	20,033	98.01

The frequency deviation of the system under two different loading conditions considered and simulated are tabulated as shown in Table 7.4. It is clear from the Table 7.4 that the maximum and minimum deviation of the system under two loading conditions simulated are 0.28 % and 0.02 %. The Discrete PLL based control logic implementation of inverter maintained the frequency of system with in the limits of 50 $\pm$ 1 Hz [278].

TABLE 7.4: Frequency deviation of the system under two different loading conditions

Load Condition / Frequency deviation	Negative Frequency deviation		Positive Frequency deviation	
	Value	(%)	Value	(%)
Constant load with Real time data of environmental conditions	49.86	0.28	50.01	0.02
Varying load with Real time data of environmental conditions	49.96	0.08	50.03	0.06

7.3.2.3 Increasing Load Pattern

The load in the PV-Wind hybrid power system is gradually increased in steps from 8 kW to 16 kW and the performance of the control technique is investigated. The DC Bus-Bar acts as input to the inverter and the simulated DC voltage, current and power input to the inverter are shown in Figure 7.15. It can

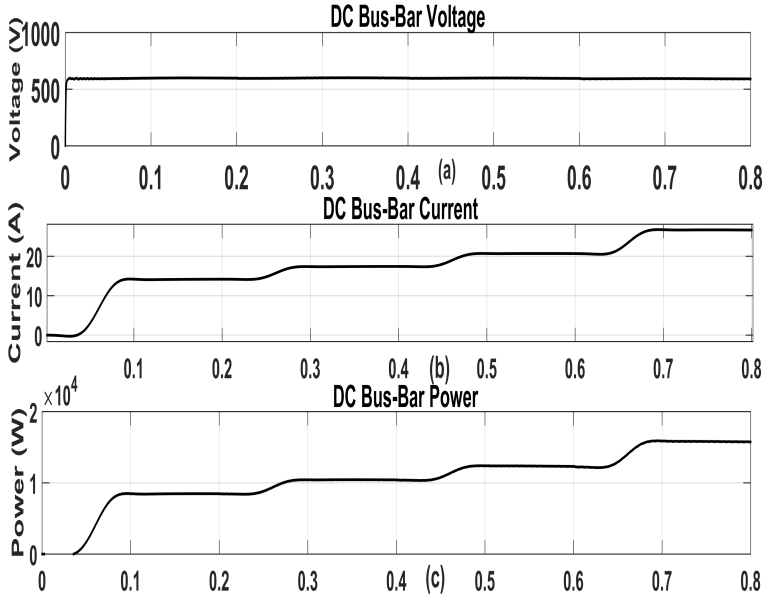

FIGURE 7.15: a) DC Bus-Bar Voltage, b) DC Bus-Bar Current, c) DC Bus-Bar power

be comprehended from Figure 7.15 that the fuzzy implementation of MPPT controlled boost converter maintained the DC bus-bar voltage at 600 V constant irrespective of change in environmental condition and load condition thereby ensuring power flow in the system. The simulated AC load voltage, current, and frequency are plotted in Figure 7.16, Figure 7.17 and Figure 7.18 respectively.

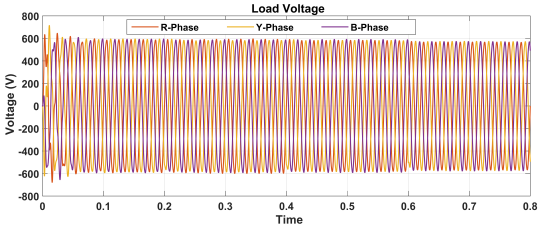

FIGURE 7.16: Simulated Load Voltage

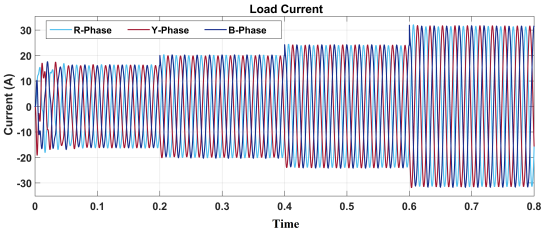

FIGURE 7.17: Simulated Load Current

From Figure 7.16 it can be observed that the load voltage remains constant at 590 V maximum value and 417 V RMS value with respect increasing pattern of the resistive load from 8kW, 10kW, 12kW

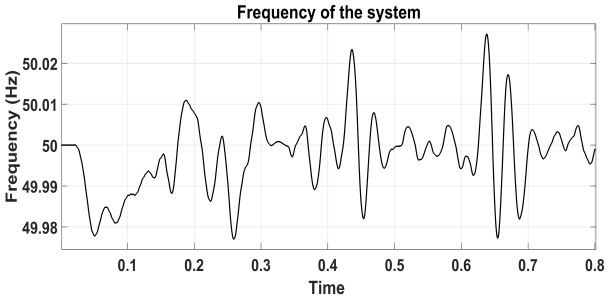

FIGURE 7.18: Simulated Frequency of the system under increasing load pattern

and 16kW which can be observed by a change in load current drawn in Figure 7.17. The Frequency of the system under increasing load pattern is within the grid code with the maximum frequency of 50.025Hz and minimum of 49.975 Hz as shown in Figure 7.18. The allowed frequency deviation according to the grid code is 49.7 – 50.2 Hz. The control implementation is showing a better frequency control with less than 2% deviation. The Total Harmonic Distortion (THD) of the system is analyzed for both voltage, current and tabulated as shown in Table 7.5. It can be comprehended that the THD of the load voltage and current from the inverter has a tremendous reduction.

TABLE 7.5: THD for Increasing Load Pattern

	THD (Before Filtering)	THD (After Filtering)
Voltage	63.68%	1.52%
Current	8.12%	1.91%

7.3.2.4 Decreasing Load Pattern

The PV-Wind hybrid power system is tested for decreasing load pattern from full load of 16 kW to 8 kW in steps. This pattern of the load is considered to investigate the performance of the control logic implementation of voltage regulated inverter to maintain the load voltage and frequency constant irrespective of change in environmental conditions. The simulated DC voltage, current and power input to the inverter are plotted in Figure 7.19. From the Figure 7.19(a) it can be comprehended that the DC bus-bar voltage is maintained constant at 600 V irrespective of change in environmental and load

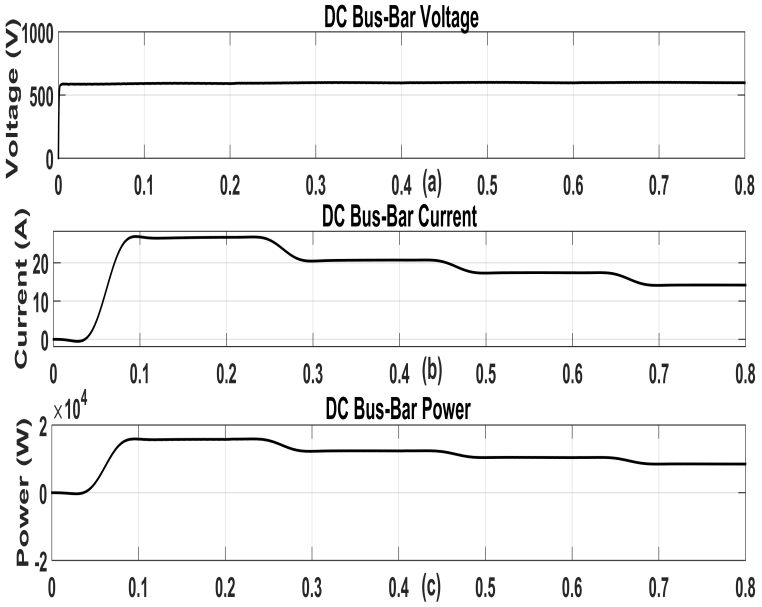

FIGURE 7.19: Simulated Frequency of the system under increasing load pattern

conditions. From Figure 7.19 (b), (c) represents DC bus-bar current and power. The simulated AC load voltage, current, and frequency of the system are plotted below.

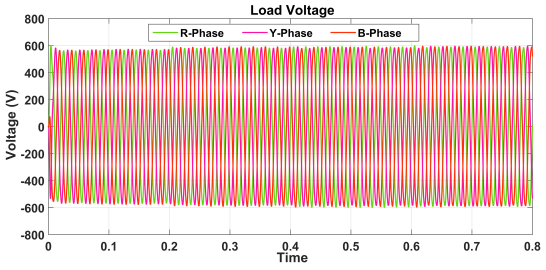

FIGURE 7.20: Simulated Load Voltage

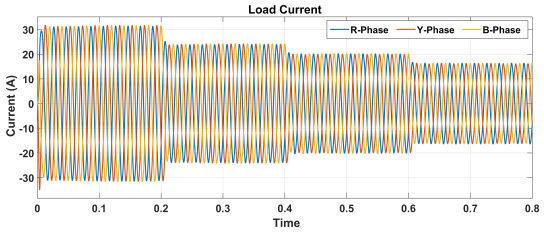

FIGURE 7.21: Simulated Load Current

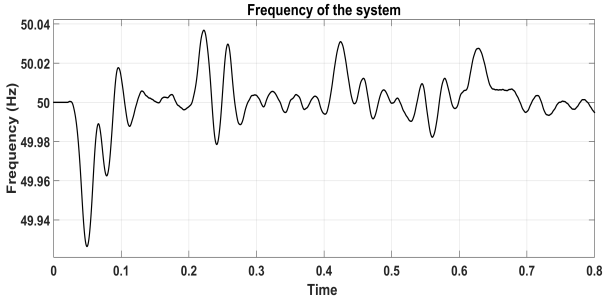

FIGURE 7.22: Simulated Frequency of the system under increasing load pattern

From Figure 7.20 it can be observed that the load voltage remains constant at 590 V maximum value and 417 V RMS value with respect increasing pattern of a load from 16kW, 12kW, 10kW and 8kW which

can be observed by a change in load current drawn in Figure 7.21. The Frequency of the system under increasing load pattern is within the grid code with the maximum frequency of 50.037Hz and minimum of 49.935 Hz as shown in Figure 7.22. The allowed frequency deviation according to the grid code is 49.7 – 50.2 Hz. The control implementation is showing a better frequency control with less than 2% deviation. The Total Harmonic Distortion (THD) of the system is analyzed for both voltage, current and tabulated as shown in Table 7.6. It can be comprehended that the THD of the load voltage and current from the inverter has a tremendous reduction.

TABLE 7.6: THD for decreasing load pattern

	THD (Before Filtering)	THD (After Filtering)
Voltage	62.64%	1.8%
Current	9.77%	2.04%

A mathematical model of PV-Wind hybrid system is presented with a two-diode model of PV cell and PMSG based generation. A 20 kW PV-Wind hybrid system is implemented in the MATLAB, Simulink. The real-time data of solar irradiation, wind speed are measured at BITS-Pilani, Hyderabad campus is utilized as the input to the PV-Wind hybrid system. A P&O, HCS MPPT tracking algorithm is used for PV, Wind-based generation to control the duty cycle of the boost converter. The performance of FLC-based MPPT controlled boost converter and Voltage regulated inverter are investigated for PV, Wind based generation individually and interconnected PV-Wind hybrid power system for varying load conditions. In interconnected PV-Wind hybrid power system, a common DC bus-bar with 600 V is formed and this DC voltage acts as input to the voltage regulated inverter. A voltage regulated inverter is implemented in order to control the output AC voltage at 415 V, 50 Hz. A discrete PLL based control logic is proposed to control the AC output voltage of the inverter.

The performance analysis of the voltage regulated inverter is tested under four different resistive loading conditions. It can be concluded that the proposed control logic operates as desired and the AC output

voltage of the PV-Wind hybrid system is maintained constant at desired level of 415 V and the system frequency is maintained within the frequency deviation is 49.93 to 50.05 Hz.

7.3.2.5 Constant resistive load with 4 KW induction motor with variable load torque

The load on the PV-Wind hybrid system with a constant resistive load with 4 KW induction motor with variable torque, the load torque is varied in steps of 10, 14, 18, 20, 12 N-m in order to check the effectives of the control to maintain the output voltage and frequency with in the grid code. The real time data of solar irradiation, wind speed of a particular day are plotted in Figure 7.6, Figure 7.7 respectively is utilized for the simulation. The simulated load voltage, load current and Frequency are shown in Figure 7.23, Figure 7.24 and Figure 7.25 respectively. The mechanical torque applied to the induction motor is shown in Figure 7.26.

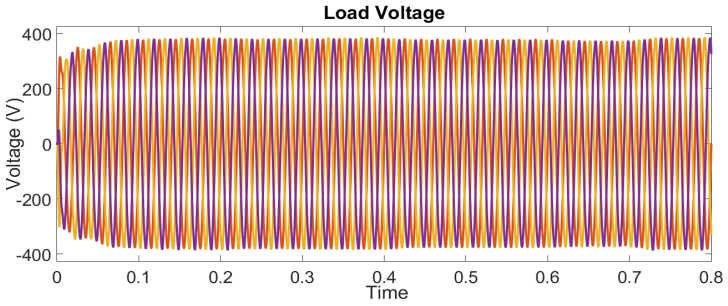

FIGURE 7.23: Simulated Load Voltage

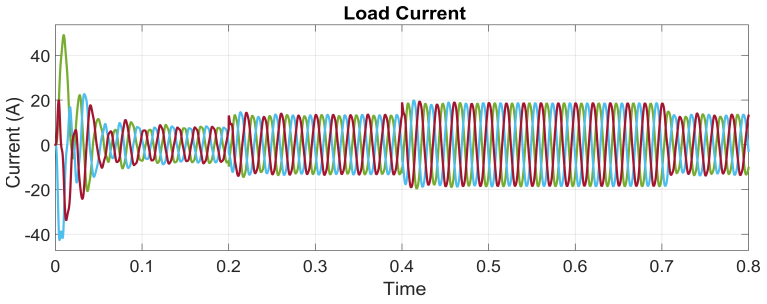

FIGURE 7.24: Simulated Load current

It can be clearly comprehended that the load voltage remained constant irrespective of change in load torque on induction motor. The change in load on PV-wind hybrid system can be observed in the

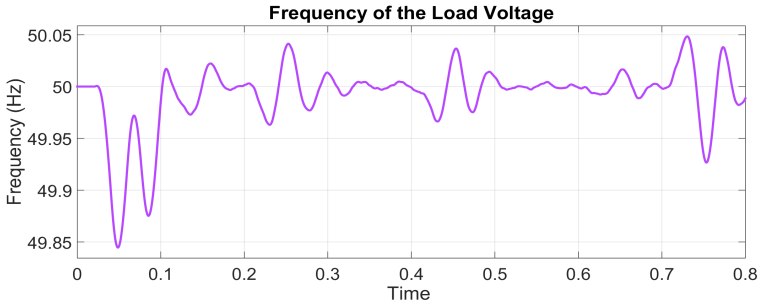

FIGURE 7.25: Simulated Frequency

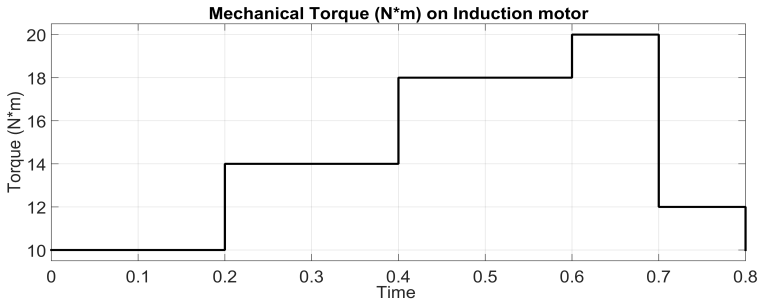

FIGURE 7.26: Mechanical Torque

load current plot i.e. Figure 7.24. The induction motors draws large amount of current while starting one it starts current drawn is normalized this phenomenon can be observed, as the load torque changes in steps the current draw is also changed. The proposed control logic of the inverter is working as desired. The proposed discrete PLL based control scheme operates as desired by maintaining the load voltage and frequency constant thereby making the system more reliable, efficient. Future Droop characteristics based LFC of for the PV-Wind Hybrid Power system will be studied in detail.

7.4 Droop Characteristics based LFC of Autonomous PV-Wind Hybrid Power System

A generation can be modeled in relation with frequency, power and droop settings as (7.3), (7.4)

$$\frac{\Delta_f}{f_n} = -R_x \frac{\Delta P_{mx}}{P_{nx}} (or) \frac{\Delta P_{mx}}{P_{nx}} = -K_x \frac{\Delta_f}{f_n} \tag{7.3}$$

$$\Delta P_{mx} = -K_x P_{nx} \frac{\Delta_f}{f_n} \tag{7.4}$$

where Δf is the change in frequency allowed, f_n is the nominal frequency of the system in Hz, R_x is the droop setting for x^{th} generation units, ΔP_{mx} is the change in power, P_{nx} is the nominal power of the x^{th} generating units. The droop R_x can be computed by (7.5)

$$R_x = \frac{\Delta f}{\Delta P} = \frac{\frac{f_{max} - f_{min}}{f_r}}{\frac{P_{max} - P_{min}}{P_r}} \tag{7.5}$$

where ΔP is the relative change in active power; f_{max}, f_{min} are the minimum and maximum frequency of the load; P_{min}, P_{max} are the minimum and maximum conditions of load power; f_r, P_r are the reference frequency, power of the generating system. The overall power change ΔP_g in the generation system can be expressed as (7.6)

$$\Delta P_g = \sum_{x=1}^{n} P_{mx} = -\frac{\Delta f}{f_n} \sum_{x=1}^{n} K_x P_x \tag{7.6}$$

Under steady state condition the balance between the power generated P_g and the system load P_l including the losses in the system occurs and expressed as (7.7)

$$P_g = \sum_{x=1}^{n} P_{mx} = P_l \tag{7.7}$$

In order to compute the steady state characteristics of the system in relation with the dependency of change in power generated with respect to frequency variation for x operating generators is by dividing (7.6) by P_l and is expressed as (7.8) or (7.9).

$$\frac{\Delta P_g}{P_l} = -\frac{\sum_{x=1}^{n} K_x P_{mx}}{P_l} . \frac{\Delta f}{f_n} = -K_g \frac{\Delta f}{f_n} \tag{7.8}$$

$$\frac{\Delta f}{f_n} = -R_g \frac{\Delta p_g}{P_l} \tag{7.9}$$

where R_g=$\frac{1}{K_g}$ is the system droop, K_g is the system stiffness factor which determines the frequency variation of the system with the change in load demand. The above droop characteristics analysis of power system can also be derived using the system characteristics of the power generation system demand P verses the frequency of the system f as graphically represented in Figure 7.27. The system balance

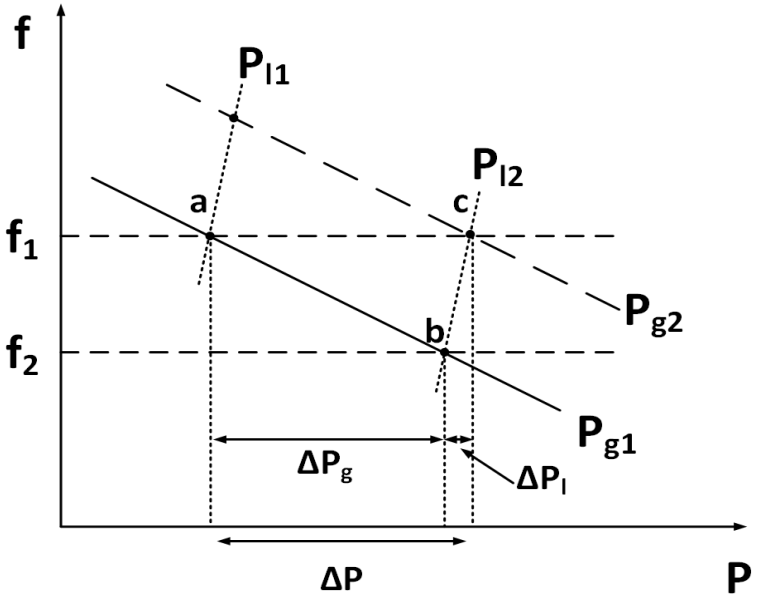

FIGURE 7.27: Graphical representation of Power system generation characteristics

occurs at the intersection point of load power demand P_l and generated power P_g. Let the system be operating at point 'a' with a load demand of P_{l1}, power generation P_{g1} and frequency f_1 as shown in Figure 7.27. With the increase in load demand the power system characteristics shifts from P_{g1} to P_{g2} and the new equilibrium point for the system is shifted to 'b' due to which the system operating frequency becomes f_2. The change in frequency $\Delta f = f_1 - f_2$ due to increase in load demand as a result generated power has to be increased by ΔP_g. Due to decrease in frequency the active power generated is decreased by ΔP_l the overall change in power in terms of change in frequency can be computed as (7.10) [142].

$$\Delta P = \Delta P_g - \Delta P_l = -(K_g + K_l) P_l \frac{\Delta f}{f_r} = -K_s P_l \frac{\Delta f}{f_r} \tag{7.10}$$

$$\frac{\Delta P}{P_l} = -K_s.\frac{\Delta f}{f_r} \tag{7.11}$$

In order to bring back the system to desired frequency f_1 the generation has to be increased by Δp_l and the transition operation of the system has to be done with the minimal frequency oscillation and this can be achieved by incorporating droop characteristics control into the control logic of Voltage regulated inverter. The block diagram of the control strategy is shown in Figure 7.28.

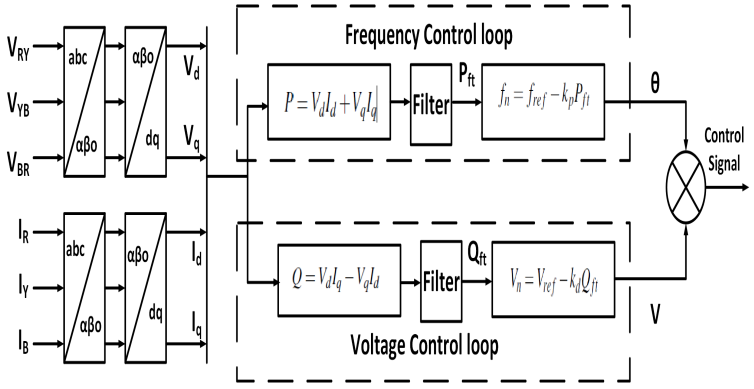

FIGURE 7.28: Block diagram of droop based LFC control technique

The three phase load voltage (V_{LL}), load current (I_L) are sensed and sensed voltage, current are transformed from *abc* to $\alpha\beta o$ expressed as (7.12) where X can be voltage or current.

$$\begin{bmatrix} X_\alpha \\ X_\beta \\ X_o \end{bmatrix} = \sqrt{\frac{2}{3}} \begin{bmatrix} 1 & \frac{-1}{2} & \frac{-1}{2} \\ 0 & \frac{\sqrt{3}}{2} & -\frac{\sqrt{3}}{2} \\ \frac{1}{\sqrt{2}} & \frac{1}{\sqrt{2}} & \frac{1}{\sqrt{2}} \end{bmatrix} \begin{bmatrix} X_a \\ X_b \\ X_c \end{bmatrix} \tag{7.12}$$

The $\alpha\beta o$ transformation are transformed into *dqo* co-ordinates as expressed in (7.13).

$$\begin{bmatrix} X_d \\ X_q \\ X_o \end{bmatrix} = \begin{bmatrix} cos\omega t & sin\omega t & 0 \\ -sin\omega t & cos\omega t & 0 \\ 0 & 0 & 0 \end{bmatrix} \begin{bmatrix} X_\alpha \\ X_\beta \\ X_0 \end{bmatrix} \tag{7.13}$$

The active and reactive power can be computed by (7.14),(7.15)

$$P = V_d I_d + V_q I_q \tag{7.14}$$

$$Q = V_d I_q - V_q I_d \tag{7.15}$$

The variation of active power is directly depend on the frequency deviation and the reactive power variation depends upon voltage variation. In order to control the power flow to maintain the load frequency instantaneous power is computed (7.14),(7.15).A low pass filter is employed to eliminate high frequency components and the filtered active power P_{ft}, reactive power Q_{ft} are utilized to compute control signal to generate nominal frequency f_n, nominal voltage V_n for controlling the output voltage and frequency expressed as (7.16),(7.17).

$$f_n = f_{ref} - k_p P_{ft} \tag{7.16}$$

$$V_n = V_{ref} - k_d Q_{ft} \tag{7.17}$$

where k_p, k_d are computed as

$$k_p = \frac{\Delta f}{P_{max}}; k_q = \frac{\Delta V}{Q_{max}} \tag{7.18}$$

With the knowledge of above mathematical modeling the LFC control strategies for PV-Wind hybrid power system is implementation in MATLAB, Simulink and the controller action is investigated for the different loading condition.

7.4.1 Simulation Results and Discussion

A 20 kW PV-Wind hybrid system with 15 KW PV generation, 5 KW Wind generation is developed in MATLAB, Simulink. To analyze the performance of control logic, the PV-Wind hybrid power system is

simulated for three distinct loading conditions

(i) Constant resistive load of 20 kW,

(ii) Deceasing load pattern from full load,

(iii) Increasing load pattern to full load, and

(iv) a detail analysis of Varying load pattern.

7.4.1.1 Constant resistive load of 20 kW

The LFC strategy of PV-Wind hybrid system developed in MATLAB, Simulink is tested for a constant load condition. The simulated load voltage, current, frequency are graphically illustrated in Figures 7.29, 7.30, 7.31. It can be clearly apprehended from Figure 7.29 that the PV-Wind hybrid power system is operating at full load, the peak value of load voltage is 565 V i.e 400 V_{rms}. The Figure 7.30 shows the load voltage, current of the system with droop based control technique. It can be observed that the PV-Wind hybrid system is operating at a load voltage of 590 V i.e 417 V_{rms}. The Figure 7.31 shows frequency of the system, it can be comprehended that the droop based control strategy has a precise LFC over the PLL based LFC. The RES generation is an equation base model and the system is loaded before it attains steady state operation due to which spikes in the frequency can be observed. once the system reaches steady state the Droop based control maintains the frequency without any steady state error as compared to the PLL based control.

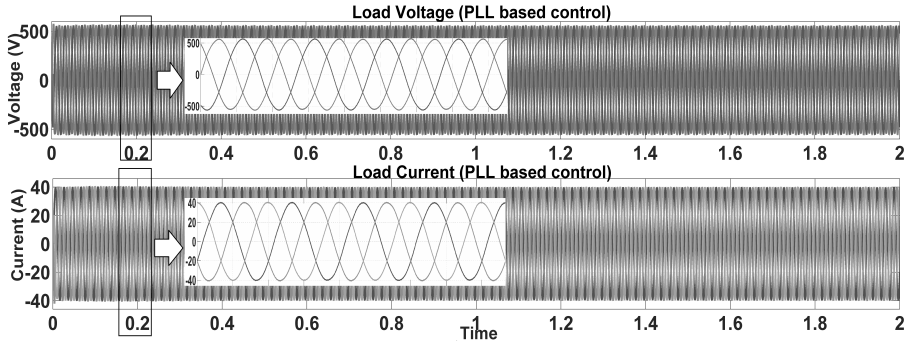

FIGURE 7.29: Load Voltage, Current for the PLL based control

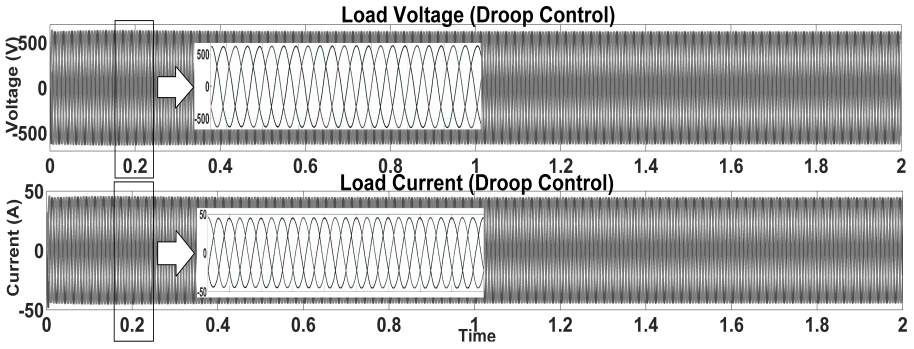

FIGURE 7.30: Load Voltage, Current for the Droop based control

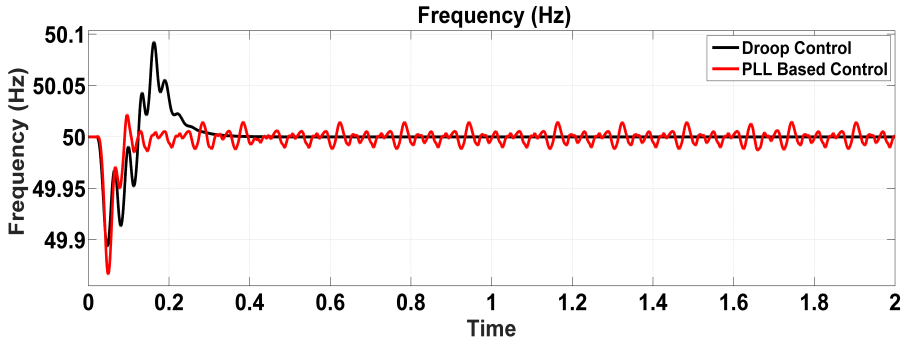

FIGURE 7.31: Frequency of the system under constant load

7.4.1.2 Decreasing load pattern from full load

The LFC designed is tested for change in load condition from full load 20 kW to 8 kW resistive load in steps of 4 kW per 0.2 sec. The decrease in load is considered to investigate the performance of the control strategy to maintain the system voltage and frequency constant when the load is thrown off suddenly. The simulated results of Load Voltage, current and frequency of the system are shown in Figures 7.32, 7.33, 7.34. From the Figures 7.32, 7.33 it can be comprehended that the load voltage gradually increased from 400 V_{rms} to 415 V_{rms} for PLL-based control, whereas the load voltage was maintained constant at 417 V_{rms} by droop based control strategy. From Figure 7.34 it can be observed that the droop base control logic brings the system frequency back to desired frequency without any steady state error for every instance of load change. whereas the PLL based control logic cannot attain a steady state.

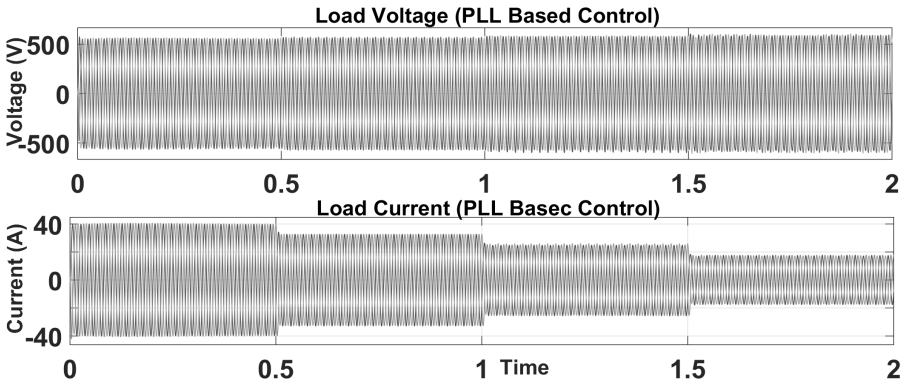

FIGURE 7.32: Load Voltage, Current for the PLL based control

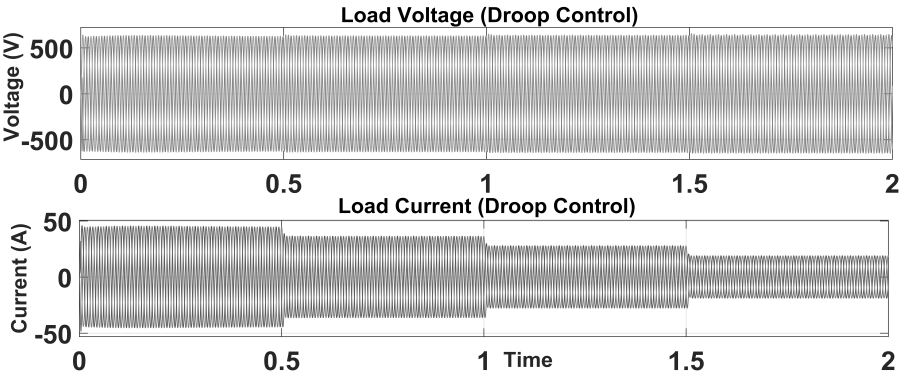

FIGURE 7.33: Load Voltage, Current for the Droop based control

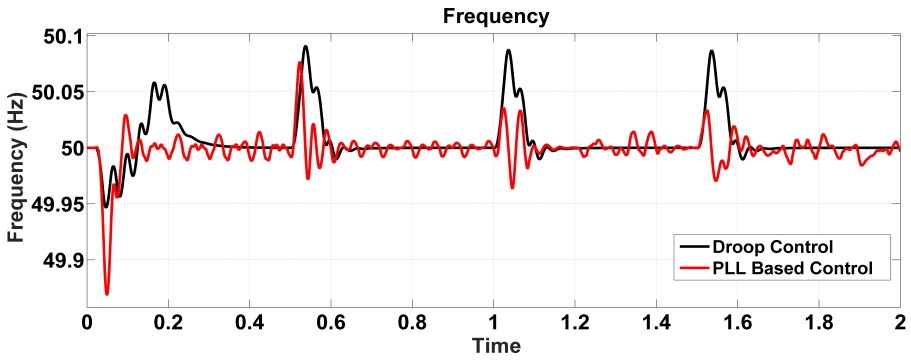

FIGURE 7.34: Frequency of the system under decreasing load pattern

7.4.1.3 Increasing load pattern to full load

The performance of control strategies is investigated to maintain the load voltage and frequency constant under increasing load pattern from 8 kW to 20 kW resistive load in steps of 4 kW per 0.2 sec respectively. This condition is inspected as the load demand increase the power generated from the PV-Wind hybrid system increases and the ability of the controller to maintain constant voltage and frequency during load

transition is investigated.The simulated results of Load Voltage, current, and frequency of the system with two control strategies are shown in Figure 7.35, 7.36, 7.37 respectively. It can be clearly observed that the load voltage and frequency of the system with droop control has accurate control in maintaining the output voltage constant at 590 V peak value i.e. $417V_{rms}$ as compared with the PLL based control, the load voltage has decreased from $415V_{rms}$ to $400V_{rms}$ is observed in Figure 7.35 and, Figure 7.36. The ability to bring back the system frequency to desired value i.e. 50 Hz after change in load condition without any steady state error is achieved better in droop based control as compared with the PLL based control. When load on the system is increased suddenly, the frequency of the system tend to decreases momentarily. From Figure 7.37 it can be comprehended that the frequency of the system designed with droop based control behaves as desired but the system with PLL-based control exhibits behavior quite opposite to the desired condition, it can be observed by increase in the frequency at instance of increase in load. So. it can be comprehended that the droop based control has better and precise control over PLL base control.

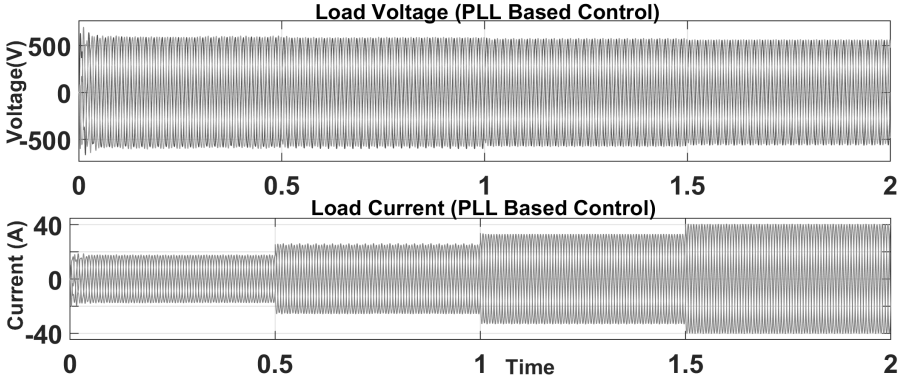

FIGURE 7.35: Load Voltage, Current for the PLL based control

7.4.1.4 Varying Resistive load pattern

To analyze the performance of LFC implemented using Droop based characteristics and Discrete PLL based control, the PV-Wind hybrid power system is simulated with a variable environmental condition and resistive load pattern. Initial load on the system is 8kW and gradually increasing the load in steps of 4 kW

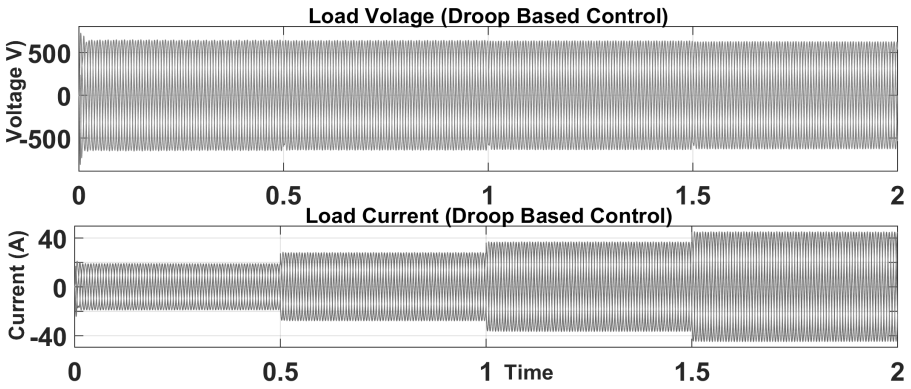

FIGURE 7.36: Load Voltage, Current for the Droop based control

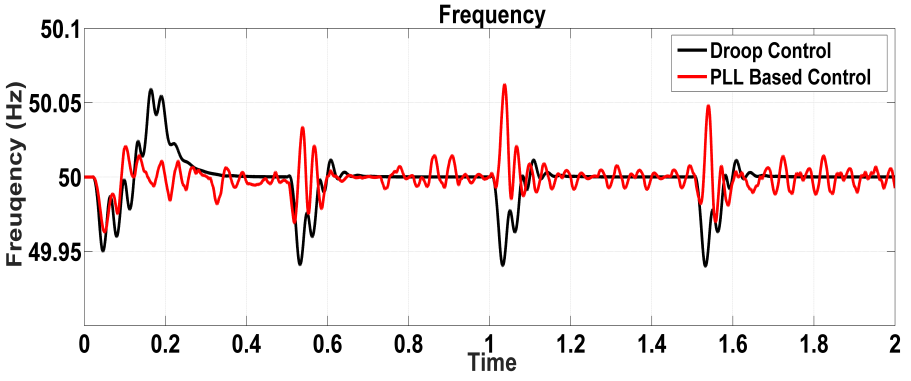

FIGURE 7.37: Frequency of the system under increasing load pattern

till the full load of 20 kW and vice-versa. The DC power input to the inverter are measured and plotted in Figure 7.38, Figure 7.39 for Discrete PLL and Droop based LFC implementation respectively. The control logic of Discrete PLL based control technique is based on voltage control and Droop based control is designed based on power control scheme to maintain output voltage. It can comprehend that DC Bus-Bar voltage is maintained constant at 600V irrespective of change in load condition and droop characteristics based control has better power flow control. The output of the inverter is pulse width modulated (PWM) AC and is plotted in Figure 7.40, Figure 7.41 for both the control technique implementation. A sinusoidal output voltage is obtained by filtering the inverter output voltage with an LC filter and the output line voltage measured between R-Y phases is plotted in Figure 7.42, Figure 7.43 for both the control logic implementation respectively. The Total Harmonic Distortion (THD) of the inverter output voltage, current for both control techniques are tabulated in Table 7.7 and both the system exhibits tremendous reduction of voltage and current THD.

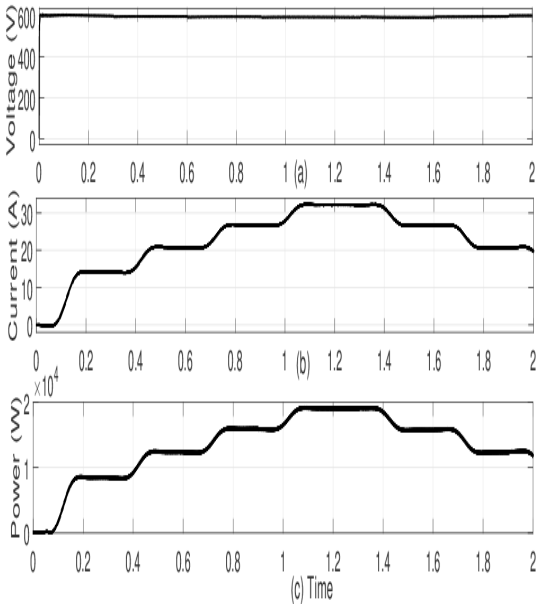

FIGURE 7.38: DC Bus-Bar Voltage, Cur- rent, Power Measurement for Discrete PLL LFC

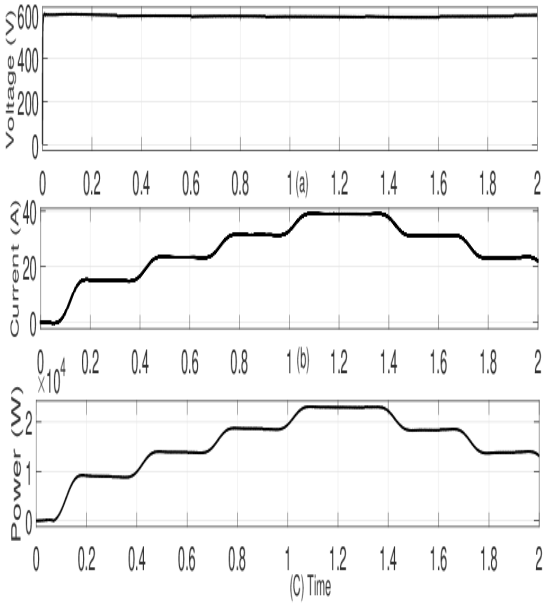

FIGURE 7.39: DC Bus-Bar Voltage, Cur- rent, Power Measurement for Droop based LFC

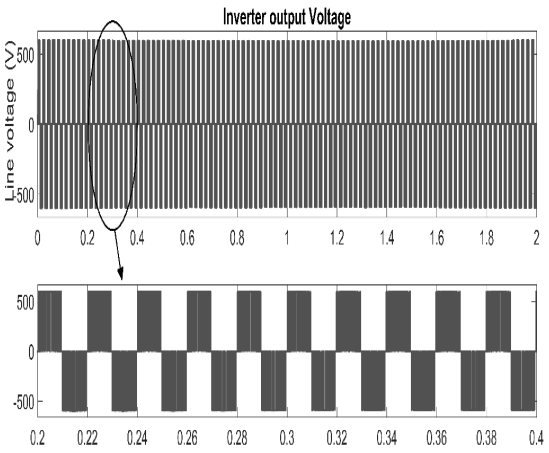

FIGURE 7.40: Inverter output voltage for Discrete PLL LFC

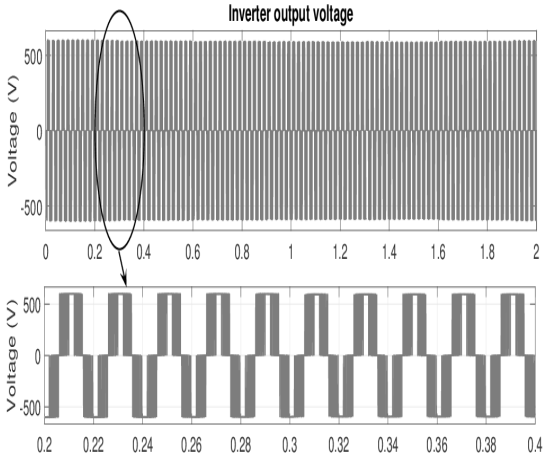

FIGURE 7.41: Inverter output voltage forDroop based LFC

It can be comprehended from Figure 7.41 that the output line voltage has a variation of 590 V to 554 V (maximum value) i.e. 417 V to 392 V (RMS) and from Figure 7.43 the output line to line voltage remains constant at 600V (maximum value) i.e. 424 V (RMS). The droop based control shows enhanced output voltage control under varying load condition as compared with discrete PLL based control. The three phase load voltage and load current for both the control techniques are plotted in Figure 7.44 to Figure 7.47.

From Figure 7.44, Figure 7.45 it can be comprehended that the droop based control has a better

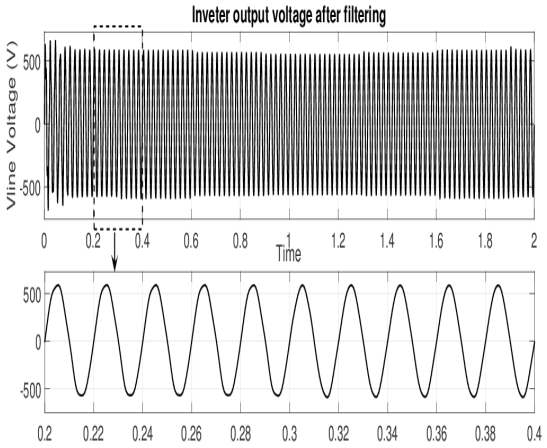

FIGURE 7.42: Inverter output voltage for Discrete PLL LFC

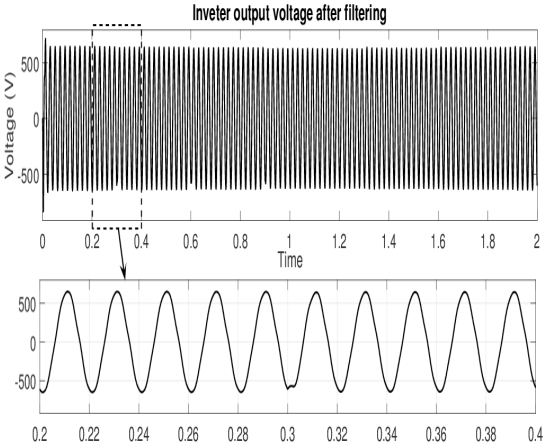

FIGURE 7.43: Inverter output voltage forDroop based LFC

TABLE 7.7: THD analaysis of the system

	Before Filter		After Filter	
	Voltage (% THD)	Current (% THD)	Voltage (% THD)	Current (% THD)
Discrete PLL based control	63.30	13.05	2.50	3.19
Droop Characteristics based Control	52.88	12.21	2.43	2.27

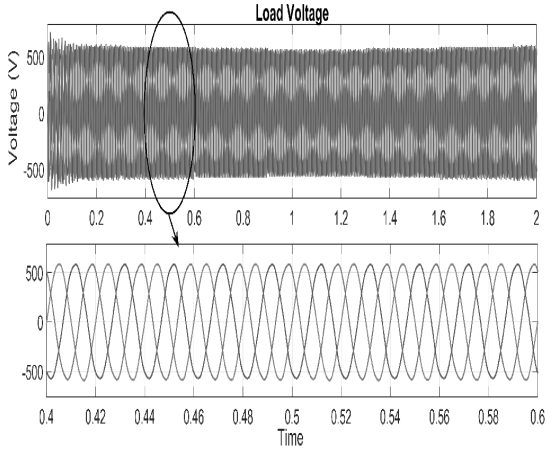

FIGURE 7.44: Three phase load voltage for Discrete PLL LFC

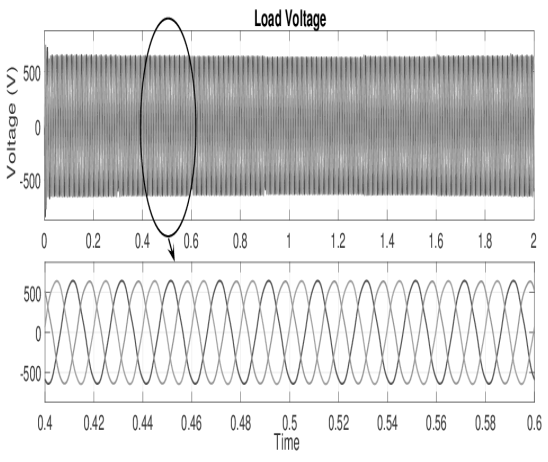

FIGURE 7.45: Three phase load voltage for Droop based LFC

control over the Discrete PLL based control in maintaining the load voltage constant irrespective of load condition. The current drawn by the load is graphically represented in Figure 7.46 and Figure 7.47. Droop based control shows enhance power flow control from source to load. A comparative plot of the frequency for both the control techniques of the system is plotted in Figure 7.48.

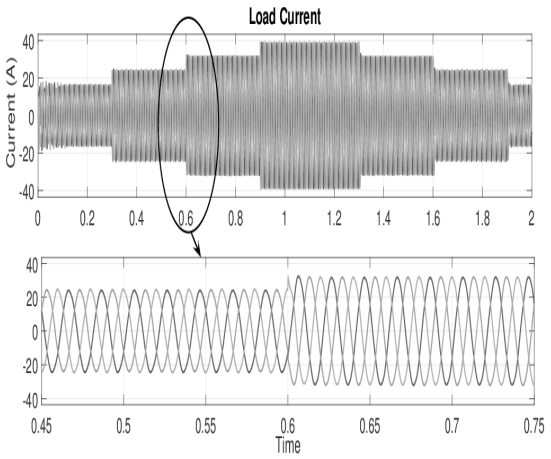

FIGURE 7.46: Three phase load current for Discrete PLL LFC

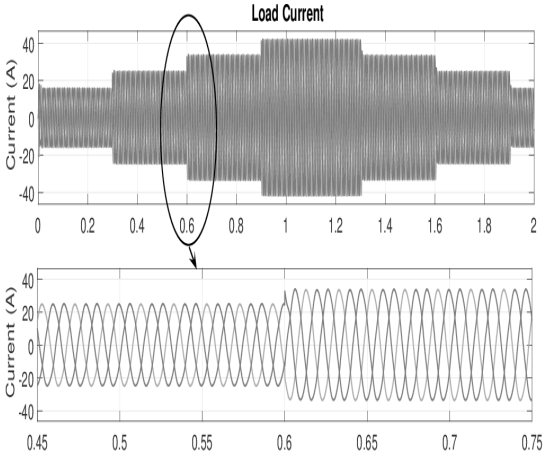

FIGURE 7.47: Three phase load current for Droop based LFC

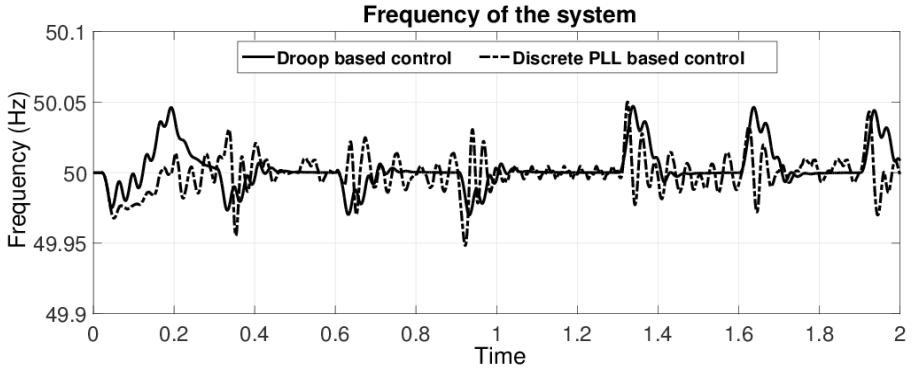

FIGURE 7.48: A Comparative plot of frequency of the system

From the Figure 7.48, it can be comprehended that the Droop based control has better load frequency control over Discrete PLL based control. The frequency of the system after a change in load condition is brought back to 50 Hz and remains constant at 50 Hz with the droop based control whereas Discrete PLL based control has a steady state error and the frequency of the system is oscillating around 50 Hz. The performance of the inverter under different loading conditions is tabulated in Table 7.8. The input to the inverter is the DC power output from PV-wind hybrid system and the output of inverter is AC power fed to the load. The input DC voltage, current, power are tabulated in Table 7.8 for the simulation time of 0.0 sec to 1.6 sec, the load is increased by 4kW every 0.3 sec starting from 8kW till it reaches maximum load 20 kW and from 1.3 sec to 2 sec the load is decreased by 4kW every 0.3 sec. From Figure 7.48 and Table 7.8, it can be comprehended that Droop based control has better voltage and frequency control over Discrete PLL based control as the voltage of the autonomous PV-Wind hybrid power system was

maintained constant at 424 V and frequency at 50 Hz under varying load condition.

7.5 Summary:

A mathematical modeling of 20 kW PV-Wind hybrid power system consisting of 15 kW PV generation in combination with 5 kW of wind power generation system operating in stand-alone mode is established. A P& O and HCS MPPT algorithms were utilized to track the MPP of PV and wind-based generation forming a 600 V DC common bus. The DC voltage is converted to AC using a voltage regulated inverter. The frequency of the system is maintained constant using LFC. The LFC of the system is investigated with two different control strategies namely PLL based control and Droop characteristics based control. Henceforth a MATLAB, Simulink model of PV-Wind hybrid system is developed to investigate the performance analysis of the LFC strategies under varying environmental conditions and resistive load pattern.

The desired operating voltage of the three phase PV-Wind hybrid system is 415 V_{rms} and the system operating frequency is 50 Hz$\pm$1%. The load voltage is maintained constant at 424V_{rms} by droop based control where the load voltage variation of 392 to 417V_{rms} is observed in Discrete PLL based control. The load frequency of the system under different loading conditions is brought back to 50 Hz without any steady state error by Droop based control techniques whereas the frequency of the system has a ripple band for Discrete PLL based control. The Droop based LFC technique exhibits better voltage, frequency and power flow control irrespective of load condition. It can be concluded that the Droop characteristics based control scheme have a better Load frequency control over Discrete PLL based LFC.

Further The Droop characteristics based LFC technique is utilized for the implementation of Tie-line frequency bias control of Interconnected PV-Wind hybrid power system.

AC Load Frequency Control of the Proposed PV-Wind hybrid power system in stand-alone mode is investigated in this chapter. Two control techniques were proposed:

TABLE 7.8: Performance of the inverter under different loading conditions

Time (s)	0.0 - 0.3		0.3 - 0.6 & 1.9 - 2.0		0.6 - 0.9 &1.6 - 1.9		0.9 - 1.3		1.3 - 1.6	
	Discrete PLL based control	Droop Characteristics based Control	Discrete PLL based control	Droop Characteristics based Control	Discrete PLL based control	Droop Characteristics based Control	Discrete PLL based control	Droop Characteristics based Control	Discrete PLL based control	Droop Characteristics based Control
Inverter Input										
Voltage (V)	600	600	600	600	595	600	590	600	595	600
Current (A)	14.1	15	20.8	23.0	26.9	30.8	32.2	38.9	26.8	30.8
Power (W)	8,460	9,000	12,480	13,800	16,000	18,500	18,998	23,340	15,946	18,500
Inverter Output										
Voltage (V)	417	424	414	424	407	424	392	424	406	424
Current (A)	11.67	11.8	17	18.4	22.4	24.9	27.9	29.7	22.6	24.7
Power (W)	8,429	8,666	12,190	13,513	15,790	18,286	18,943	21,811	15,893	18,139
Efficiency (%)	99.6	96.3	97.7	98.0	98.6	98.8	99.7	94.0	99.6	98.0

1. Discrete PLL,

2. Droop Characteristics based control.

The proposed control techniques were investigated for a different pattern of load changes in the system with real time data of solar illumination and wind speed. From the study, it is comprehended that the Droop characteristics based LFC control exhibit enhanced control over Discrete PLL based LFC. The next chapter will focus on analyzing the performance of grid-connected PV-Wind hybrid power system. Further investigating the tie-line frequency control of the Interconnected two-area PV-Wind hybrid power system.